Available online at www.sciencedirect.com
SCIENCE DIRECT®

Polymer 46 (2005) 12218–12225

polymer

www.elsevier.com/locate/polymer

Polypyrrole materials doped with weakly coordinating anions: influence of substituents and the fate of the doping anion during the overoxidation process

Sébastien Gentil [a], Eulalia Crespo [a,1], Isabel Rojo [a], Aurélie Friang [a], Clara Viñas [a], Francesc Teixidor [a,*], Bohumír Grüner [b], Detlef Gabel [c]

[a] Institut de Ciència de Materials de Barcelona (ICMAB/CSIC), Campus de la UAB, 08193 Bellaterra, Spain
[b] Institute of Inorganic Chemistry, Academy of Sciences of the Czech Republic, 250 68 Rez near Prague, Czech Republic
[c] Department of Chemistry, University of Bremen, P.O. Box 330 440, D-28334 Bremen, Germany

Received 14 July 2005; received in revised form 18 October 2005; accepted 20 October 2005
Available online 14 November 2005

Abstract

The influence of weakly coordinating anions with different shapes and substituents has been studied to get the overoxidation resistance limit of the material, ORL. The anions utilized are derivatives of $[Co(C_2B_9H_{11})_2]^-$, $[B_{12}H_{12}]^{2-}$ and $[B_{12}H_{11}NH_3]^-$. The following tendencies have been established (1) boron cluster monoanions are to date the anions that offer the highest stability to overoxidation of PPy doped materials (2) the ORL stability of the material can not be attributed only to the shape of the cluster (3) monoanionic clusters are far superior than dianionic to get an ORL rise (4) cluster charge density reduction results in ORL rise as has been observed in $[Co(C_2B_9H_{11})_2]^-$ after incorporation of electron-withdrawing substituents with no electron back-donation (5) globular, rigid and large monoanions are less suitable for enhanced ORL values than elongated and non-rigid species (6) adequate anion's substitution produce a rise in the ORL of the material, thus polyether side-arms are beneficial with $[Co(C_2B_9H_{11})_2]^-$, whereas, T-shaped methylaryl groups are appealing in $[B_{12}H_{11}NH_3]^-$ based materials, respectively, (7) substituents on the anions usually imply higher difficulty in the materials' growth. The high boron contents in these materials has permitted to learn on the fate of the doping anions during the overoxidation process. There is a built-up of the concentration of the doping anion in the electrolyte near surface area, whereas, a depletion is observed in the nearest inner layers.

Keywords: Overoxidation; Polypyrrole; Borane

1. Introduction

Since their discovery 25 years ago, the development of conducting organic polymers (COP) combining organic polymer and semi-conducting electronic properties continues unabated [1,2]. Polypyrrole is one of the COPs most widely investigated regarding its potential applications [3] especially in sensors [4,5], actuators [6–8] or as electrochromic devices [9] among others. Polypyrrole materials (PPy) are reasonably stable in air, present high conductivity, good electrochemical properties and thermal stability and are easily generated both chemically and electrochemically [10]. For practical applications, long-term stability of the material towards repetitive oxidation/reduction cycling or towards exposition to high anodic potential for short periods of time is of primary interest. The PPy chemical stability limit is known to be related to the overoxidation resistance limit (ORL) of the material, beyond which the conducting material properties are definitely lost [11,12]. It is generally accepted that during the PPy degradation process, nucleophiles usually attack the polymer double-bond alternating system, generating carbonyl groups, and producing the loss of the conductivity [13–16]. In the PPy electropolymerization, anions from the solution are inserted into the polymer matrix to maintain the material's electroneutrality, neutralizing the positive charges generated on the oxidized polymer threads [3]. Therefore, the nature of the counter-ion used in the electropolymerization and the applied experimental conditions play a very important role in the resulting properties of the PPy films [17–19]. In the search for new properties, many investigations have been conducted on polypyrrole doped with different anions such as $[ClO_4]^-$ [20],

---

* Corresponding author. Tel.: +34 93 580 18 53; fax: +34 93 580 57 29.
E-mail address: teixidor@icmab.es (F. Teixidor).
[1] Eulalia Crespo is enrolled in the UAB PhD program.

0032-3861/$ - see front matter © 2005 Elsevier Ltd. All rights reserved.
doi:10.1016/j.polymer.2005.10.092

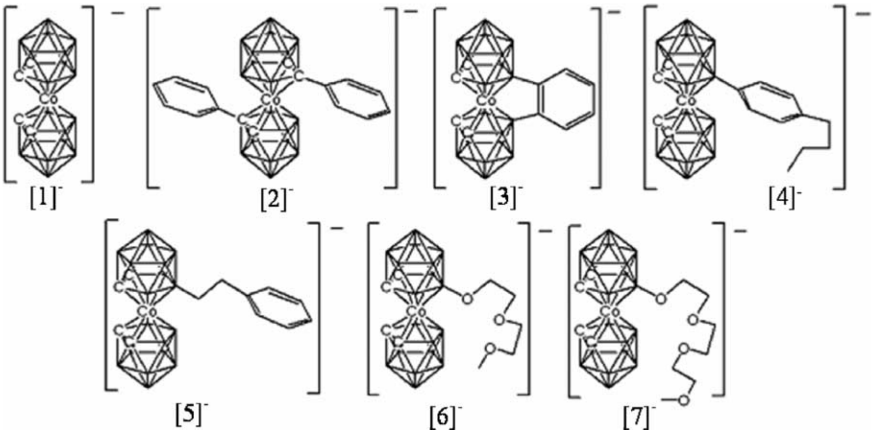

Chart 1. $[Co(C_2B_9H_{11})_2]^{-}$, $[1]^{-}$ and its derivatives $[2]^{-}$–$[7]^{-}$. All plain vertexes are BH units. Vertexes simply named C stand for CH.

$[BF_4]^{-}$ [21], $[PF_6]^{-}$ [22], $[NO_3]^{-}$ [23], $[Cl]^{-}$ [23], surfactants [24] and even with unusual counter-ions like heteropolyanions [25] such as $[SiW_{12}O_{40}]^{4-}$ or phosphotungstate [26] $[PW_{12}O_{40}]^{3-}$, among others. Weakly coordinating anions provide interesting properties in the fields where they are applied [27]. In particular weakly coordinating anions based on boron clusters have been successfully applied in many areas [28]. With the objective to study the convenience of using weakly coordinating anions derived from borane clusters in COPs we initiated the study on PPy [19,29]. Boron clusters appear to be very appropriate for this task due to their compact but not globular shape, the existence of exo hydride groups, and their low charge density. Interestingly $[CB_{11}H_{12}]^{-}$, the paradigm of the weakly coordinating carborane anions did not provide improved results with regard to conventional anions. Indeed $[CB_{11}H_{12}]^{-}$ and $[B_{10}Cl_{10}]^{2-}$ PPy doped materials gave ORLs up to 1090 and 890 mV vs. Ag/AgCl (10% KCl), respectively, values that are comparable to other data reported for common anions [29]. A definitive improvement in the ORL of PPy was found with the cobaltabisdicarbollide metallacarborane (Chart 1, $[1]^{-}$). This anion of formula $[Co(C_2B_9H_{11})_2]^{-}$ leads to a PPy material with an ORL of 1270 mV, practically 300 mV higher than previously studied PPy doped materials [19]. It is our interpretation that the elongated shape of $[Co(C_2B_9H_{11})_2]^{-}$, its low charge density and the spatial distribution of electron rich B–H groups which are hypothesized to interact with PPy positive charges should certainly be determinant in increasing the ORL. In this report we are presenting a thorough study of derivatives of $[Co(C_2B_9H_{11})_2]^{-}$ and the dinegative cluster $[B_{12}H_{12}]^{2-}$, $[8]^{2-}$, see Charts 1 and 2, to substantiate the above explanations in the unusual stabilization caused by $[1]^{-}$. These studies are complemented with monoanionic amino derivatives [30] of $[8]^{2-}$, Chart 2, in which there exists a dinegative cluster with a diffuse charge and a monopositive tail with hydrophobic groups.

These investigations emphasize the relevance of the B–H containing anions in enhancing the ORL of the PPy materials. Important improvements of the ORL values have been observed with the two series of borane anions studied, derivatives of $[Co(C_2B_9H_{11})_2]^{-}$ and $[B_{12}H_{11}NH_3]^{-}$. Divalent borane anions do not improve the ORL. Electronic effects in the sense to remove electron density from the cluster are proven to be relevant. Flexible side chains have produced the most overoxidation resistant materials for $[B_{12}H_{11}NH_3]^{-}$ derivatives, whereas, polyether side chains have produced the best in the $[Co(C_2B_9H_{11})_2]^{-}$ series. By XPS analysis assisted with Ar sputtering it has been possible to demonstrate the depletion of doping anions in inner regions of the material and the accumulation in near surface areas for PPy materials oxidized near the ORL of the material.

2. Experimental section

2.1. Chemical and reagents

Pyrrole was purchased from Aldrich, distilled under reduced pressure before its use and stored under nitrogen at 0 °C in dark. The cobaltabisdicarbollide derivatives $NMe_4[3,3'-Co(1-C_6H_5-1,2-C_2B_9H_{10})_2]$ ($NMe_4[2]$) [31], $NMe_4[8,8'-\mu(1'',2''-C_6H_4)-3,3'-Co(-1,2-C_2B_9H_{10})_2]$ ($NMe_4[3]$) [32], $Cs[3,3'-Co(8-(1''-(4''-C_4H_9)-C_6H_4)-1,2-C_2B_9H_{10})(1',2'-C_2B_9H_{11})]$

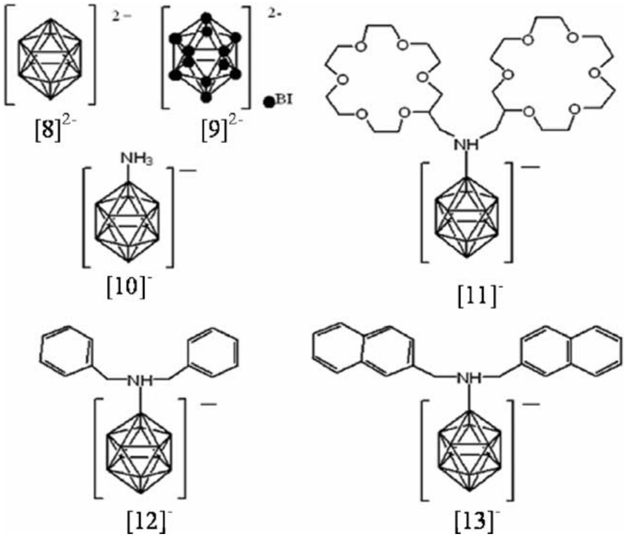

Chart 2. $[B_{12}H_{12}]2^{-}$, $^{[8]}{}_{2}^{-}$, and its derivatives $^{[9]}{}_{2}^{-}$–$[13]^{-}$. All plain vertexes are BH units. Vertexes with a dark circle correspond to BI.

(Cs[4]) [33], Cs[3,3′-Co(8-($C_2H_4C_6H_5$)-1,2-$C_2B_9H_{10}$)(1′,2′-$C_2B_9H_{11}$)] (Cs[5]) [33], Na[3,3′-Co(8-(OCH_2CH_2)$_2$$OCH_3$-1,2-$C_2B_9H_{10}$) (1′,2′-$C_2B_9H_{11}$)] (Na[6]) [34], Na[3,3′-Co(8-(OCH_2CH_2)$_3$$OCH_3$-1,2-$C_2B_9H_{10}$)(1′,2′-$C_2B_9H_{11}$)] (Na[7]) [34], were synthesized as reported in the literature. Cs[Co($C_2B_9H_{11}$)$_2$] (Cs[1]) and $Cs_2[B_{12}H_{12}]$ (Cs[8]) were provided by Katchem Ltd, Prague. Salts of $[N(CH_3)_4]_2[B_{12}I_{12}]$ ($N(CH_3)_4$[9]), $[N(CH_3)_4][B_{12}H_{11}NH_3]$ ($N(CH_3)_4$[10]), Cs[*N*,*N*-1-((18-crown-6)CH_2)$_2$$NHB_{12}H_{11}$] (Cs[11]), Cs[1-($C_6H_5CH_2$)$_2$$HNB_{12}H_{11}$] (Cs[12]) and $[N(CH_3)_4]$[1-($C_{10}H_7CH_2$)$_2$$HNB_{12}H_{11}$] ($N(CH_3)_4$[13]) were synthesized following reported procedures [30,35].

2.2. Electrosynthesis of the polymer films

Electrolyte solutions for polypyrrole film preparations were deoxygenated by bubbling nitrogen gas during 10 min before use. All electrochemical experiments were done using an EG&G Princeton Applied Research model 273 A potentiostat-galvanostat. Polypyrrole films were synthesized from acetonitrile solutions (1% water) of 0.1 M pyrrole and 3.5×10^{-2} M of the doping anion with a standard three-electrode double compartment cell, on a 3 mm diameter glassy carbon plate working electrode and a 10 cm platinum wire as counter electrode. Polypyrrole films were grown using both galvanostatic (at 0.5 mA during 225 s) and cyclic voltammetry (at 100 mV/s from −1000 to 2000 mV, 30 scans) techniques. Potentials are reported with respect to Ag/AgCl (0.1 M tetrabutylammonium chloride in CH_3CN) reference electrode for the organic medium and Ag/AgCl (10% KCl) for the aqueous medium. PPy/[8] and PPy/[10] were electropolymerized in aqueous solution.

2.3. Electrochemical characterization

Polypyrrole ORL tests were carried out by Linear Sweep Voltammetry (LSV) in a 0.1 M NaCl distilled water solution in a single-compartment cell. Membranes were exposed to a low voltage scan rate (0.5 mV s^{-1}, 0–1800 mV) after a careful wash in CH_3CN and then in distilled water. The estimation of the ORL values was complemented with cyclic voltammetry (CV) at 100 mV s^{-1} from −1300 to 1000 mV in NaCl 0.1 M.

2.4. Scanning electron microscopy (SEM) and X-ray photoelectron spectroscopy (XPS)

Samples were prepared on stainless steel plates (1 cm^2) at 3 mA for 15 min with the solutions having the same concentrations as specified above. An Hitachi S530 scanning electron microscope was used to examine the PPy morphology. For X-ray photoelectron spectroscopy analysis a PHI ESCA-5500 assisted with argon plasma sputtering was used.

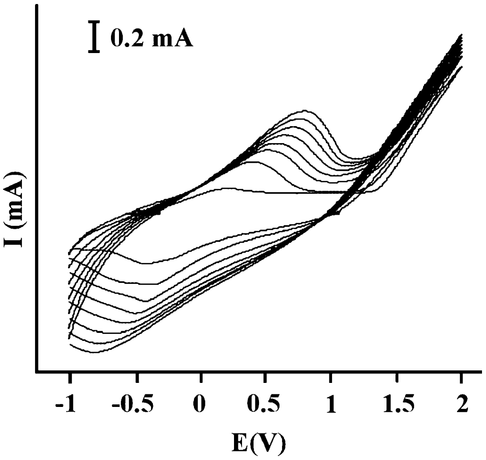

Fig. 1. Sequential cyclic voltammetry for the electropolymerization of PPy/[4] in CH_3CN at 100 mV s^{-1} from −1000 to 2000 mV. From the 2nd to the 30th scan, every fourth is shown for a better clarity.

3. Results and discussion

3.1. Cobaltabisdicarbollide derivatives

3.1.1. Electrochemical growing properties of the doped polypyrroles

A similar growth behavior was observed for all PPy/[1]–[7] materials irrespective of the synthetic procedure, either galvanostatically or by CV methods. Differences are found, in the latter method, for the intensity data. The PPy/[4] CV trace growth after thirty sequential scans is shown in Fig. 1, as a representative example.

For all PPy/[1]–[7] synthesized by CV, the first anodic scan show a strong wave with an onset potential corresponding to the pyrrole ring oxidation. A fact of notice is that not-so-well defined anodic and cathodic peaks in the CVs as for the derivatives of $[1]^-$ are observed when common doping anions such as $[ClO_4]^-$ or $[PF_6]^-$ are used.

Fig. 2 displays the CV intensity of the anodic peak vs. the number of scans for PPy/[1]–[7]. A higher intensity is obtained after each new scan, but the increase depends on the side groups on $[1]^-$. The highest speed of growth is found with PPy doped with $[1]^-$, followed by $[4]^-$ and $[5]^-$ then by $[2]^-$ and $[3]^{-\cdot}$ The materials with less tendency to grow are these with doping anions $[6]^-$ and $[7]^-$, their growth is one order of magnitude smaller than for PPy/[1]. This last result is in agreement with PPy/[3,3′-Co(8-C_4H_4N–(CH_2)$_2$–O–(CH_2)$_2$–O-

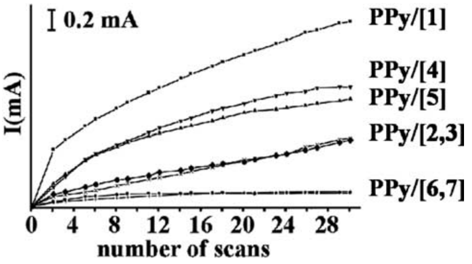

Fig. 2. Anodic wave current intensity vs. number of scans for PPy/[1]–PPy/[7].

$1,2\text{-}C_2B_9H_{10})(1',2'\text{-}C_2B_9H_{11})]$, a self-doped copolymer [36] whose current intensity was far from the normal $[1]^-$ doped material. From Fig. 2 it is then observed that sets of materials can be arranged depending on the substituents on $[1]^-$.

3.1.2. Relationship between overoxidation stability and the structure of the doping anions

Three major differences are found in the anions shown in Chart 1. In complex $[2]^-$ substituents are on C, thence there are as many B–H sites available as in $[1]^-$. In complex $[3]^-$, the benzene substituent blocks two boron positions, producing two B–H sites less than in $[1]^-$. Finally, complexes $[4]^-$–$[7]^-$ have the substituent on one boron, then having one B–H less than in $[1]^-$. It is to be noticed that the boron on which the substitution takes place in $[4]^-$–$[7]^-$ corresponds to the electron richest B–H site in $[1]^-$. Besides these electronic considerations complexes $[1]^-$–$[7]^-$ evidence shape differences. In this regard, complexes $[2]^-$ and $[3]^-$ are more globular than the other. As a last consideration, complexes $[6]^-$ and $[7]^-$ incorporate oxygen donor atoms as a possible binding group of cations.

Overoxidation measurements were made by the LSV technique in NaCl 0.1 M and are displayed in Fig. 3 for all PPy/[1]–[7] materials. The LSV peak for PPy/[1] at 1270 mV sits in the middle of the different LSV traces. The rigid $[2]^-$ and $[3]^-$ dopants produce less overoxidation resistant materials, with LSV peaks at 1210 and 1150 mV, respectively. Compound $[4]^-$ produces equal ORL than $[1]^-$ at 1270 mV. Finally, PPy/[5], PPy/[6], PPy/[7], present ORL values at 1330, 1410, 1450 mV, respectively. The PPy/[7] potential shift value of 180 mV vs. PPy/[1] implies that $[7]^-$ is the most overoxidation stabilizing anion tested in our experimental conditions and reported so far in the $[Co(C_2B_9H_{11})_2]^-$ family. The structural differences in the tested anions may provide some hints on the reasons for this different behavior. Before starting a comparative discussion we feel necessary to outline some characteristics of $[1]^-$. This anion has a rigid cylindrical shape with the longer axis being 10.2 Å, this value is given including the two most opposite hydrogen atoms and is comparable to the near 12 Å expected for the PPy bipolaron. Additionally it has a three-dimensional disposition of the BH's and cation/BH interactions have been described in the literature [37–39] involving different BH sites. A possible consequence of this is that PPy positive charges interact with cluster BH bonds, thereby increasing the overoxidation capacity of the material. This explanation seems reasonable taking into account that when several BH positions are substituted as is the case for $[Co(C_2B_9H_8X_3)_2]^-$, X = Cl, Br, less overoxidation resistant materials are found [29].

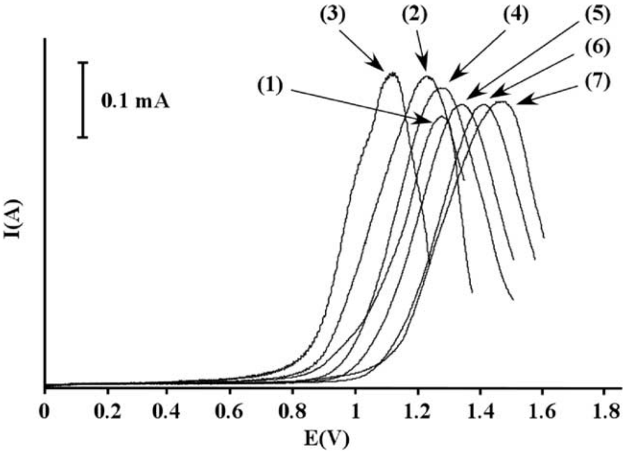

Fig. 3. Overoxidation current vs. applied potential for PPy/[1]–PPy/[7].

The fundamental characteristics of $[1]^-$ are also present in $[2]^-$–$[7]^-$. This explains why the electrochemical properties of the different materials are close to these found for PPy/[1]. However it seems clear that large and rigid volume fragments, e.g. aryls, are non-desirable. Conversely less rigid alkyl or alkoxy groups such as these in $[5]^-$–$[7]^-$ improve the overoxidation performance of the materials. An alternative electronic explanation can also be given in the aim to benefit from a low charge density anion [19]. Aryl groups withdraw electron density from the cluster but at the same time compensate this lost by electron back-donation [33]. Other chains, even the alkyl one when bonded to boron, only remove electron density from the cluster producing an anion with even less electron density. That $[3]^-$ should be the worst doping anion seems clear from the above explanations: it is rigid, would be the one with the highest electron density and is the one that has less B–H units. Anion $[2]^-$ is the one that stresses better the negative influence of radial rigid groups. It has the same characteristics as $[1]^-$ but incorporates two phenyl groups on cluster carbon atoms. Compounds $[4]^-$–$[7]^-$ present the same geometrical characteristics, but differ on the substituents. One of the dicarbollide fragments in the complexes is free of substituents while the second moiety is substituted at the B(8) position. Differences between PPy/[5] and PPy/[7] ORL values can arise from the electron-withdrawing strength of the chain substituents, the coordinating capacity of oxygen atoms and the chain lipophilicity. Anions $[5]^-$–$[7]^-$ which have a similar side chain seem to suggest that the possibility of metal coordination by the oxygen atoms may be a desirable property. Indeed PPy/[6] and PPy/[7] present the best overoxidation resistant materials. The alkoxy organic groups of complexes $[6]^-$ and $[7]^-$ could either participate in the compensation of the PPy positive charges by electrostatic interactions or in regulating the mobility of cations within the material in a similar way as oxygen atoms do in $[3,3'\text{-}Co(8\text{-}X\text{-}(CH_2CH_2O)_2\text{-}1,2\text{-}C_2B_9H_{10})(1',2'\text{-}C_2B_9H_{11})]$ coordinating to Na or hard cations [34,40–42]. As a further evidence of the relevance of having anions with weaker charge density, we have tested $[3,3'\text{-}Co(8\text{-}CH_3)\text{-}1,2\text{-}C_2B_9H_{10})(1',2'\text{-}C_2B_9H_{11})]^-$ [36]. In this anion the side chain is shorter than in $[5]^-$. If the electronic factors, but not the steric, are the dominant ones, similar ORLs would be found for PPy/$[3,3'\text{-}Co(8\text{-}CH_3)\text{-}1,2\text{-}C_2B_9H_{10})(1',2'\text{-}C_2B_9H_{11})]$ and PPy/[5]. Indeed this is what is observed: ORL values of 1.34 and 1.33 V are measured.

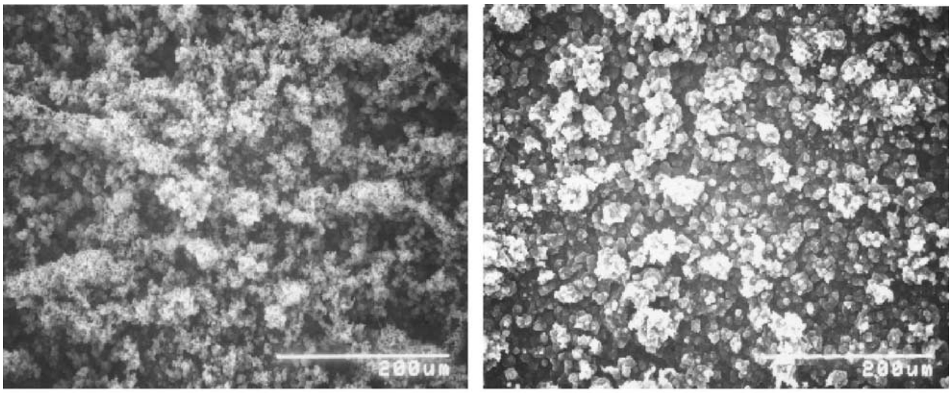

A B

Fig. 4. SEM images of electropolymerized PPy/[3] (A) and PPy/[7] (B).

3.1.3. Electron microscopy observation

Fig. 4 shows micrographs of the best and the worst overoxidation resistant materials, PPy/[7] (Fig. 4(B)) and PPy/[3] (Fig. 4(A)). A micrograph of PPy/[1] has already been reported [43]. As observed in the Fig. 4(A) more homogeneous surface is observed for PPy/[7] than for PPy/[3]. This could be an structural consequence of the higher difficulty to produce a compact arrangement caused by the large and rigid anion $[3]^-$.

3.2. Dodecaborates derivatives

In the aim to apply the results drawn from derivatives of $[1]^-$ to other anions not having the same shape we have chosen anions $[8]^-$–$[13]^-$ as doping elements for other PPy materials. See Chart 2. As an important feature these anions also incorporate B–H groups. For the $[8]^{2-}$–$[13]^-$ anions two main classifications can be produced: one that accounts for the charge which includes $[8]^{2-}$–$[9]^{2-}$ as divalent anions and $[10]^-$–$[13]^-$ as monoanions, and a second set that accounts for large bifurcated substituents. In the latter, one set includes $[8]^{2-}$–$[10]^-$ and the second $[11]^-$–$[13]^-$. Following the conclusions drawn from the derivatives of $[1]^-$, the divalent anions, including the bulky $[9]^{2-}$, should produce less overoxidation resistant materials than the very similar monovalent partners. On the other hand it was expected that the behavior of the bifurcated anions would be comparable to the one observed for PPy/[5]–[7]. Synthetic protocols are as indicated in Section 2.

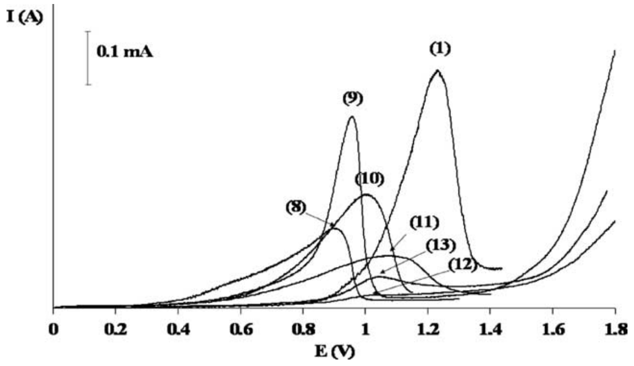

Fig. 5. Overoxidation current vs. applied potential for PPy/[8]–PPy/[13] and PPy/[1] for comparative purposes.

3.2.1. Tests based on LSV experiments

Overoxidation measurements by LSV for PPy/[1] and PPy/[8]–[13] are reported in Fig. 5. Whereas, the LSV traces for PPy/[8]–[10] are similar to these for the derivatives of $[1]^-$, those for PPy/[11]–[13] are very different. For comparative purposes the LSV for PPy/[1] has been also included in Fig. 5. As predicted PPy/[8]–[9] are materials with low ORL values. Notwithstanding so the importance of charge delocalization and charge density makes their ORL values comparable to common monovalent anions. In this way ORL values of 910 and 960 mV have been measured. For PPy/[10], the monovalent nature of the anion raises the ORL to 990 mV. It is noticeable from Fig. 5 the non-symmetric shape of the trace for PPy/[8] and PPy/[10], that corresponds to the two PPy materials obtained by electropolymerization in aqueous solution. It seems that the polymer starts at lower potentials their decomposition as a consequence of they having being prepared in water, producing a higher porosity and weaker materials [3,44]. PPy/[9] is the unique one that displays a quasi-symmetrical typically observed [19] well-defined peak. Less informative are the LSV traces for PPy/[11]–[13], PPy/[11] being the only one that resembles the typical shape found for PPy/[1]. For PPy/[11] the measured ORL value is at 1150 mV. For PPy/[12] the trace is totally different, showing a sudden but not intense rise in intensity near 900 mV. A similar trace had been observed for cobaltabisdicarbollide self-doped copolymer [36]. This is interpreted as if the material, contrarily to PPy/[1] or their derivatives, does not have a sudden degradative process. The degradation process extends over a larger range of potentials.

3.2.2. Tests based on uptake-release of cations

As the LSVs for PPy/[12] and Ppy/[13] were not providing any clue concerning the ORLs of these materials, tests based on the uptake-release of cations were conducted. The electroactivity of a PPy/[X] material doped with a non-extrudable anion can be measured observing its capacity to incorporate

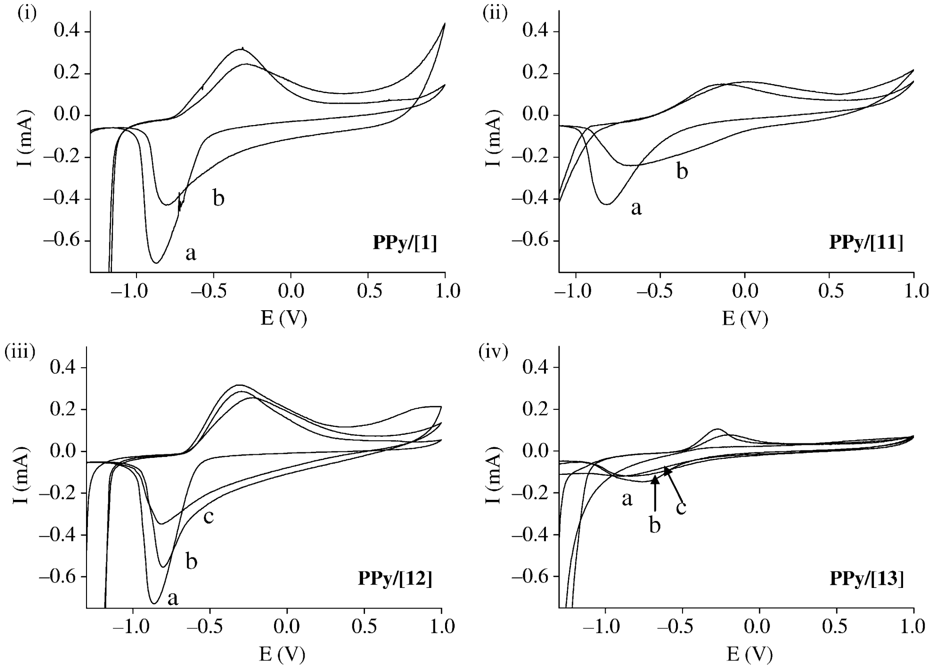

Fig. 6. Cyclic voltammograms of PPy/[1] (i), PPy/[11] (ii), PPy/[12] (iii) and PPy/[13] (iv) in NaCl (0.1 M) after anodic treatment at: (a) $E=500$ mV, (b) $E=1100$ mV, (c) $E=1700$ mV. The (c) trace is not represented for PPy/[1] and PPy[11] due to a flat signal at 1700 mV.

cations during the reduction process of the material, and its capacity to liberate them during the oxidation. If a material is insulted with increasing oxidizing potentials there will be one such that the electroactivity of the material will be banned. The minimum insulting voltage at which this banned process takes place corresponds to the ORL. To perform these studies several samples of the PPy/[X] material must be produced and each one should be treated to a determined insulting potential, E_{ox}. For PPy/[12] several electrodes have been prepared and exposed each one up to an oxidizing insulting potential by means of a LSV process, the studied voltages range from 500 to 2100 mV. After subjecting the material to a specified E_{ox}, a CV experiment is performed to test its cation exchange capacity. With no exception, the ability to uptake/release cations in an oxidizingly insulted membrane is less than in a just synthesized one. CV ion exchange voltammograms for different PPy/[12] electrode samples treated at 500, 1100, and 1700 mV, are presented in Fig. 6. With an increasing E_{ox}, a gradual decrease of both anodic and cathodic peak intensity is observed. When one PPy/[12] electrode is LSV treated up to a potential of 1700 mV, the intensity value of the CV cathodic semi-cycle decays to 50% of the maximum measure for an electrode insulted to 500 mV, but the activity of the material is still reasonable. When the LSV oxidizing tests are extented up to 1900 and 2100 mV, a dramatic drop in the cathodic and anodic intensity is found and completely flat CV curves are observed, consistent with a totally overoxidized, therefore non-recoverable material. The PPy/[12] ORL can be estimated to be near 1800 mV (Fig. 6 iii for PPy/[12]). The LSV plot shown in Fig. 5 for PPy/[13] is intermediate between this for PPy/[11] and PPy/[12]. The PPy/[13] ORL is estimated to be 1800 mV. Therefore, both [12] and [13] are the most stabilizing anions tested so far for PPy overoxidation, including the successful $[1]^-$. CV's for PPy/[1] and PPy/[11]–[13] are represented in Fig. 6 after anodic LSV treatment up to 500, 1100 and 1700 mV. The axes are equal for a better comparison. The results after treatment up to 1700 mV are not shown for PPy/[11] or PPy/[1] because at these potentials the responses are flat due to total material degradation.

3.3. What is happening in the overoxidation process?

The anions $[1]^-$–$[7]^-$ and $[11]^-$–$[13]^-$ have produced the PPy materials more resistant to overoxidation reported so far. Why is so? All of them have in common the existence of large number of B–H units in their molecules. Also, the ratio of B/C is very high in the materials generated, therefore there is a large number of B–H units per unit of pyrrole. As an example the composition of the PPy/[1] contains 4.5 B–H units per pyrrole. This ratio decreases for the $[B_{12}H_{12}]^{2-}$ derivatives to 3 B–H units per pyrrole but is still very high. This high ratio, and taking into account that no other anions have been reported that produce materials with such high ORLs, leads us to hypothesize that hydrides stabilize the moving polarons and bipolarons. The bulk composition obtained by X-ray photoelectron spectroscopy studies performed on the polymer PPy/[1] and on the copolymer PPy/[A] ($A=[3,3'\text{-Co}(8\text{-}C_4H_4N\text{–}(CH_2)_2\text{–O–}(CH_2)_2\text{–O-}1,2\text{-}C_2B_9H_{10})(1',2'\text{-}C_2B_9H_{11})]^-$) correspond to a ratio of Py to $[3,3'\text{-Co}(1,2\text{-}C_2B_9H_{10})_2]$ of 4.34 [19,36]. In order to ascertain if the chemical structure and/or the charge of the doping anions [8]–[13] would influence on the doping efficiency of the PPy materials, XPS analysis on the polymers PPy/[12] and PPy/[13] were done. A ratio of Py to anion near 6.0 was obtained. On the other hand the large number of boron atoms in these PPy materials have permitted to study for the first time the in-depth distribution of the anion in the material by XPS analysis [19]. We can benefit from this large ratio of B and from this technique to get a picture of what happens during the overoxidation.

The most obvious consequence of a PPy material doped with a non-extrudable anion when it has been subjected to high insulting anodic potentials is the loss of cation capture and cation release capacity in the CV experiment. At the limit a flat response is obtained. Therefore this test tells on the good health of the material after the anodic processing. The course of losing response is not abrupt but gradual. Subjecting a material to higher insulting anodic potentials produces a gradual decrease in the cyclic voltammetry cathodic peak Ipc, change that is also observed in the Ipa. These are the more obvious phenomenological consequences of the overoxidation, but what are the material's intrinsic details of such a process? We have studied the chemical composition depth profile of plain, anodically processed, and overoxidized samples of PPy/[12] and PPy/[13] by XPS analysis of generated new layers obtained with the assistance of argon plasma sputtering. The carbon and boron profiles for PPy/[12] are represented in Fig. 7(a) for non insulted material and in Fig. 7(b) for an insulted material up to the overoxidation potential. Oxygen profile is not represented in Fig. 7 although oxygen possibly as H_2O is present homogeneously in the material in a ratio near 0.27 with regard to boron. A minor oxygen built-up is found near the surface in non-insulted PPy/[12]. This parallels an increase in the same region of the doping agent evidenced by an increase in the boron percentage, and consequently a decrease in carbon. The carbon and boron profiles are much different in the insulted material as seen in Fig. 7(b) where the outermost doping anion built-up effect, represented as vertical lines, is so dramatic that one layer of material is dominantly made up of anions and water. Also in Fig. 7(b) is observed the draining of the doping agent in the neighboring layers indicated by horizontal lines. A similar situation is also observed for PPy/[13], although in this case the built-up and draining zones are not as well defined as for PPy/[12].

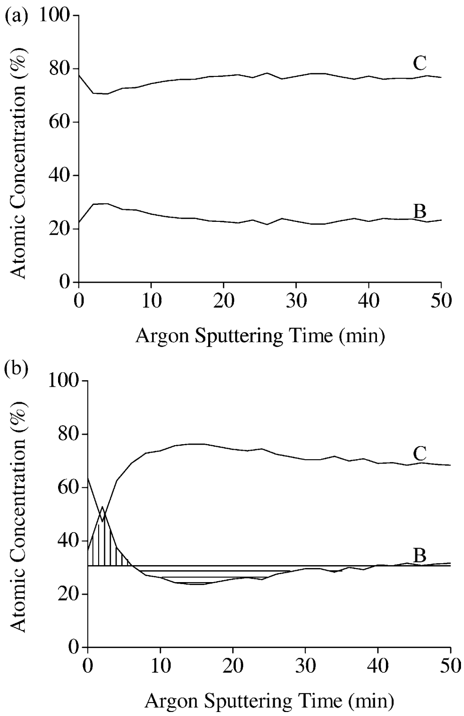

Fig. 7. Depth Atomic percentage profile of PPy/[12] in unaltered material (a), and after anodic insult to 1800 mV (b). Carbon (C) and boron (B) profiles are shown. Boron profile in curve (b) shows two different regions: in the inner layers region (horizontal stroke) Boron atomic concentration is lower than the expected for an homogeneous overoxidized film, whereas, layers close to the surface (vertical stroke) show a higher concentration. This fact can be understood as the movement of the doping anion during the overoxidation process from the inner layers to the surface and in the case of PPy/[12], as a result of its shape, an accumulation of $[12]^-$ happens.

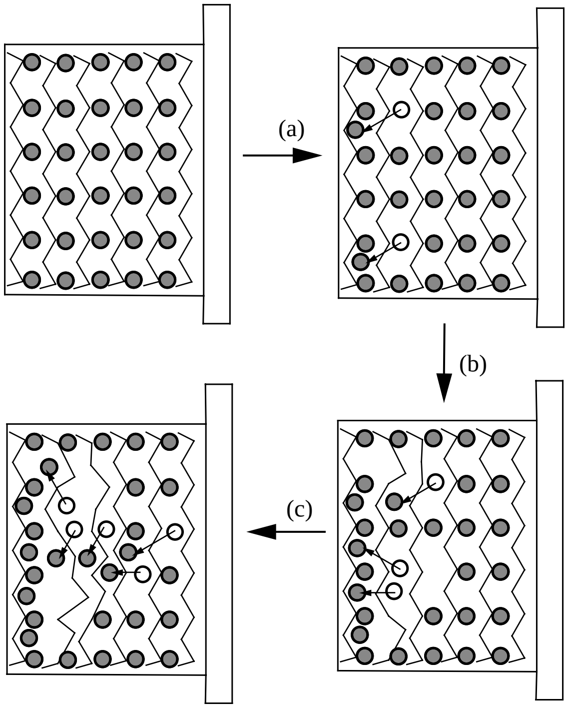

Fig. 8. The doping anion fate in a gradually oxidized PPy material. The zig-zag pattern stands for PPy threads. Full circles represent positions occupied by the doping anions. The empty circles denote previously occupied positions and the arrows indicate the trajectory to the new position.

The whole overoxidation process seems to gradually deplenish all layers of doping anions to produce a layer very close to the surface constituted by the former anions and water molecules, both probably associated through hydrogen bonds. This process is diagrammatically shown in Fig. 8.

4. Conclusions

The following considerations come out of the result of this research: (1) boron cluster monoanions are to date the anions that offer the highest stability to overoxidation of PPy doped materials. This is interpreted considering the high delocalization of charge in there cluster species, and the large abundance of BH hydride units, able to compensate the moving positive charges in the PPy strands; (2) elongate, $[Co(C_2B_9H_{11})_2]^-$, and spherical $[B_{12}H_{12}]^{2-}$ boron clusters have been utilized in this study, and the ORL stability of the material can not be attributed to the shape of the cluster itself.; (3) monoanionic clusters are far superior than dianionic in the ORL improvement. Monoanionic derivatives of $[B_{12}H_{12}]^{2-}$ have been obtained from derivatizations of $[B_{12}H_{11}NH_3]^-$; (4) the relevance of charge density reduction in the cluster for ORL improvement has been observed in $[Co(C_2B_9H_{11})_2]^-$ by incorporating electron-withdrawing substituents with no capacity for electron back-donation; (5) globular, rigid and large monoanions are comparatively less suitable for good ORL values than elongated, and non-rigid species; (6) improvement of the ORL stabilization capacity of a suitable anion can be done by adequately choosing the substituents. Polyether sidearms have been adequate for improving the ORL in $[Co(C_2B_9H_{11})_2]^-$, whereas, T-shaped methylaryl groups have been found interesting in $[B_{12}H_{11}NH_3]^-$ based materials, respectively.; (7) extra ORL stabilization by adequate choice of the substituent usually implies a higher difficulty in the materials' growth. The existence of a large ratio of boron in these materials has permitted to get information by XPS analysis supported by Ar sputtering on the fate of the doping anions during the overoxidation process. A built-up of the doping anion takes place in the electrolyte near surface area and a depletion is observed in the immediate inner layers.

Acknowledgements

This work has been supported by CICYT (MAT2004-01108) and SGR (2001/SGR/00337). Sébastien Gentil thanks the French Ministry of Foreign Affairs for a 'Lavoisier' post-doctoral grant. We thank the Institute of Inorganic Chemistry (Academy of Sciences of Czech Republic) and the Department of Chemistry (University of Bremen) for the synthesis of some of the studied anions.

References

[1] Shirakawa H, Louis WJ, MacDiarmid AG, Chiang CK, Heeger AJ. J Chem Soc, Chem Commun 1977;16:578–80.
[2] Diaz AF, Kanazawa KK, Gardini GP. J Chem Soc, Chem Commun 1979; 14:635–6.
[3] Sadki S, Schottland P, Brodie N, Sabouraud G. Chem Soc Rev 2000; 29(5):283–93.
[4] Ionescu RE, Gondran C, Gheber LA, et al. Anal Chem 2004;76(22): 6808–13.
[5] Okuno H, Kitano T, Yakabe H, et al. Anal Chem 2002;74(16):4184–90.
[6] Otero TF, Cortes MT. Adv Mater 2003;15(4):279–82.
[7] Smela E. Adv Mater 2003;15(6):481–94.
[8] Pager EWH, Smela E, Inganas O. Science 2000;290(5496):1540–5.
[9] Boehme JL, Mudigonda DSK, Ferraris JP. Chem Mater 2001;13(12): 4469–72.
[10] Wang L-X, Li X-G, Yang Y-L. React Func Polym 2001;47(2):125–39.
[11] Lewis TW, Wallace GG, Kim CY, Kim DY. Synth Met 1997;84(1-3): 403–4.
[12] Otero TF, Marquez M, Suarez IJJ. Phys Chem B 2004;108(39):15429–33.
[13] Ge H, Qi G, Kang E, Neoh KG. Polymer 1994;35(3):504–8.
[14] Palmisano F, Malitesta C, Centonze D, Zambonin PG. Anal Chem 1995; 67(13):2207–11.
[15] Jaramillo A, Spurlock LD, Young V, Brajter-Toth A. Analyst 1999; 124(8):1215–21.
[16] Christensen PA, Hamnett A. Electrochim Acta 1991;36(8):1263–8.
[17] Tang H, Kitani A, Shiotani M. Electrochim Acta 1996;41(9):1561–7.
[18] Lippe J, Holze RJ. J Electroanal Chem 1992;339(1-2):411–22.
[19] Massalles C, Borros S, Viñas C, Teixidor F. Adv Mater 2000;12(16): 1199–202.
[20] Qiu Y-J, Reynold JR. J Polym Sci, Polym Chem 1992;30(7):1315–25.
[21] Prejza J, Lundström I, Skotheim T. J Electrochem Soc 1982;129(8): 1685–9.
[22] Zhou M, Heinze J. Electrochim Acta 1999;44(11):1733–48.
[23] Yuan YJ, Adeloju SB, Wallace GG. Eur Polym J 1999;35(10):1761–72.
[24] Kim IW, Lee JY, Lee H. Synth Met 1996;78(2):177–80.
[25] Bidan G, Genies EM, Lapkowski MJ. Electroanal Chem 1988;251(2): 297–306.
[26] Takeo S, Akira O, Masaji A, Henichi H. J Chem Soc, Faraday Trans I 1988;84(11):3941–9.
[27] Krossing I, Raabe I. Angew Chem, Int Ed 2004;43(16):2066–90.
[28] Reed CA, Kim KC, Stoyanov ES, Stasko D, Tham FS, Mueller LJ, et al. J Am Chem Soc 2003;125(7):1796–804 and refs. therein.
[29] Massalles C. URL, Doctoral Thesis; 2002.
[30] Grüner B, Bonnetot B, Mongeot H. Collect Czech Chem Commun 1997; 62(8):1185–204.
[31] Viñas C, Bertran J, Gomez S, Teixidor F, Dozol J-F, Rouquette H, et al. J Chem Soc, Dalton Trans 1998;17:2849–254.
[32] Plešek J, Heřmánek S. Collect Czech Chem Commun 1995;60(8): 1297–302.
[33] Rojo I, Teixidor F, Viñas C, Kivekäs R, Sillanpää R. Chem-A Eur J 2003; 9(18):4311–23.
[34] Teixidor F, Pedrajas J, Rojo I, Viñas C, Kivekäs R, Sillanpää R, et al. Organometallics 2003;22(17):3414–23.
[35] Sivaev IB, Bregadze V, Sjöberg S. Collect Czech Chem Commun 2002; 67(6):679–727.
[36] Massalles C, Llop J, Viñas C, Teixidor F. Adv Mater 2002;14(11): 826–9.
[37] Yang X, King W, Sabat M, Marks TJ. Organometallics 1993;12(10): 4254–8.
[38] Tsang CW, Sun J, Xie Z. J Organomet Chem 2000;613(1):99–104.
[39] Chetcuti PA, Hofherr W, Liégard A, Rihs G, Rist G, Keller H, et al. Organometallics 1995;14(2):666–75.
[40] LLop J, Masalles C, Viñas C, Teixidor F, Sillanpää R, Kivekäs R. J Chem Soc, Dalton Trans 2003;4:556–61.
[41] Plešek J, Grüner B, Císarová I, Báca J, Selucký P, Rais J. J Organomet Chem 2002;657(1-2):59–70.
[42] Plešek J, Grüner B, Hermánek S, Báca J, Marecek V, Jänchenová J, et al. Polyhedron 2002;21(9-10):975–86.
[43] Masalles C, Borros S, Viñas C, Teixidor F. Adv Mater 2002;14(6): 449–52.
[44] Ko JM, Rhee HW, Park S-M, Kim CYJ. Electrochem Soc 1990;137: 905–9.